Journal of Applied Polymer Science

Flame-Retardant Olefin Block Copolymer Composites with Novel Halogen-Free Intumescent Flame Retardants Based on the Composition of Melamine Phosphate and Pentaerythritol

Zinan Zhang, Bin Lin, Ning Zhou, Fengyuan Yu, Hongbin Zhang

Shanghai Key Lab of Polymer Dielectrics, Department of Polymer Science and Engineering, Advanced Rheology Institute, School of Chemistry and Chemical Technology, Shanghai Jiao Tong University, Shanghai 200240, People's Republic of China

Correspondence to: H. Zhang (E-mail: hbzhang@sjtu.edu.cn)

ABSTRACT: A series of halogen-free intumescent flame retardants (IFR) based on home-made melamine phosphate and pentaerythritol system (MPPER) including polyamid 12, basic nickel carbonate ($NiCO_3 \cdot 2Ni(OH)_2 \cdot 4H_2O$), lanthanum oxide ($La_2O_3$), and expandable graphite compounding with MPPER, were adopted for flame retarding olefin block copolymers (OBC). Flame-retardant effects and thermal stabilities of OBC-IFR composites were investigated by limiting oxygen index, vertical burning test (UL-94), and thermogravimetry analysis along with the analysis of morphological structures of the char residue by scanning electron microscopy. The mechanical properties and the flame-retardant mechanism of the final composited materials have been also discussed. The loading of suitable amount of IFR can improve effectively the flame retardancy of the OBC with tolerable decrease in mechanical properties.
 J. Appl. Polym. Sci. **2014**, *131*, 40066.

KEYWORDS: blends; composites; polyolefins; thermoplastics; elastomers

Received 23 June 2013; accepted 13 October 2013

DOI: 10.1002/app.40066

INTRODUCTION

Thermoplastic elastomers (TPEs) are a new class of materials that behave like thermoset rubbers, possessing the advantages of processibility and convertibility via thermoplastic techniques such as blow molding, injection molding, extrusion, and thermoforming. However, the inherently high flammability limits their usage. Although the halogenated compounds are good flame-retardant additives for polymers, increasing attention is focused on halogen-free flame retardants due to the ecological problems. Metal hydroxides, such as alumina hydroxide and magnesium hydroxide, have been widely used as halogen-free flame retardants in TPEs.[1] However, to reach UL94 V-0 rating, high loading of metal hydroxides is required, which makes the filled TPEs have a high density, poor processability, and mechanical properties. In recent years, intumescent flame retardants (IFR) have been widely used in TPEs due to their advantages of little smoke release, low corrosion, no dripping during a fire, and low toxicity.[2–4] A typical IFR system is usually made up of three main substances: a dehydration catalyst for char formation (acid source), a carbon rich polyol compound (carbon source), and an organic amine or amide acting as blowing agent (gas source). During the heating process, IFR can generate a swollen multicellular char layer on the surface of the material, which protects the underlying material from the flame action, and acts as a physical barrier that limits the diffusion of combustible volatile products to the flame, and of oxygen to the polymer.[5] The concerned IFR systems have been well summarized by Wang et al.,[6] that is, ammonium polyphosphate (APP)/melamine (ME)/pentaerythritol (PER) system, APP/triazine compound system, melamine phosphate (MP)/PER system, and so on. Especially, in MPPER system, PER is the carbon source and MP acts as acid source and gas source at the same time. Despite a number of superior qualities, IFR systems have some flaws compared with halogenated flame retardants, for example, low flame-retardant efficiency.[7] To enhance the flame-retardant efficiency, synergistic agents have been widely used in IFR systems, such as zeolites,[8] magnesium oxide (MgO), ferric oxide (Fe_2O_3),[9] and so on. Many researches have shown that synergistic agents can effectively promote in catalyzing the reactions among IFR components. Expandable graphite (EG) is another effective IFR additive of polymers, which can expand in the perpendicular direction and generate a vermicular structured layer when exposed to a heat source. Unlike the typical IFR system, EG performs both as a carbon source and as a gas source.[10]

Recently, the Dow chemical company developed a class of olefin block copolymers (OBC) with new molecular architecture via chain shuttling polymerization process.[11] As a novel TPE, the OBC consist of crystallizable ethylene–octene blocks with low

comonomer content and high melting temperature (hard blocks), alternating with amorphous ethylene–octene blocks with high comonomer content and low glass transition temperature (soft blocks). Compared to statistically random ethylene–octene copolymers, these OBC exhibit a superior balance of flexibility and heat resistance as well as significantly improved compression set and elastic recovery.[12] However, to our best knowledge, their flame-retardant properties have not been explored.

In this work, a series of novel halogen-free IFR systems for OBC including polyamid 12 (PA12), basic nickel carbonate ($NiCO_3 \cdot 2Ni(OH)_2 \cdot 4H_2O$), lanthanum oxide ($La_2O_3$), and EG compounding with MPPER were studied and compared, respectively. Fourier transform infrared (FTIR), thermogravimetry analysis (TGA), limiting oxygen index (LOI), vertical burning test (UL-94), scanning electron microscopy (SEM), and tensile tests were used to evaluate the synergistic effect of the flame retardants. The flame-retardant mechanism of OBC-IFR systems was also proposed.

EXPERIMENTAL

Materials

OBC (Infuse 9817 and Infuse 9000) was provided by Dow Chemical Company. PA12 (Grilamid TR90) was obtained from EMS-Grivory Company (Switzerland). EG (#60) was bought from Shanghai Daoguan Rubber and Plastic Company (China). Melamine, PER, phosphoric acid (H_3PO_4), $NiCO_3 \cdot 2Ni(OH)_2 \cdot 4H_2O$, and La_2O_3 were purchased from Sinopharm Chemical Reagent Company (China).

Preparation

Preparation of MP. Melamine (1 mol) and phosphoric acid (1.05 mol) were added to 1500 mL water at 95°C in a 3000 mL three-necked flask. The flask was fitted with a condenser, thermometer, and stirrer. The mixture was stirred for 2 h at 95°C and formed white MP crystals. The MP crystals were filtered off and dried in oven at 100°C overnight.

Preparation of OBC/MPPER/PA12 Composites. The OBC and MPPER/PA12 IFR systems were mixed with various weight ratios in a HAAKE internal mixer (Rheocord 90, HAAKE GmbH, Germany) with a chamber volume of 60 cm^3. The mixer temperature was kept at 190°C for 20 min. A constant rotor speed of 100 rpm was applied. Then the mixed samples were compressed in sheets on a hot-stage (XLB-D, Rubber Machinery Factory, China) under a pressure of 10 MPa at 190°C.

Preparation of Other OBC-IFR Composites. The OBC and MPPER, MPPER/$NiCO_3 \cdot 2Ni(OH)_2 \cdot 4H_2O$, MPPER/$La_2O_3$, EG, and MPPER/EG IFR systems were mixed with various weight ratios in a HAAKE internal mixer at 150°C and 100 rpm for 20 min, respectively. The mixed samples were compressed in sheets under a pressure of 10 MPa at 150°C.

Characterization

FTIR Spectroscopy. The FTIR spectra of synthetic MP were recorded on a Spectrum 100 Fourier transform infrared spectrophotometer (Perkin Elmer) in the range of 4000–500 cm^{-1}.

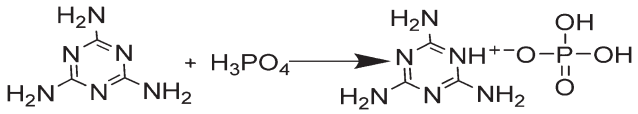

Scheme 1. The synthesis of MP.

Thermogravimetry Analysis. TGA data were obtained in nitrogen at a heating rate of 20°C/min using a TA Q5000IR thermogravimetric analyzer (TA Instrument Company, USA). All samples were measured from room temperature to 700°C under a continuous nitrogen flow.

Limiting Oxygen Index Measurements. The LOI was measured according to ASTM D2863 using an hc-2 oxygen index meter (Jiangning Analysis Instrument Company, China). The specimens for the test were of dimensions 120 × 6.5 × 3 mm^3.

Vertical Burning Tests. According to the ANSL/UL-94-2009 test standard, the vertical burn tests were performed on a CFZ-1 type instrument (Jiangning Analysis Instrument Company, China). The specimens used were of dimensions 120 × 12.7 × 3 mm^3.

Morphology Measurements. The morphology of char residue in flame-retardant OBC systems was examined by SEM (SM-7401F, JEOL, Japan). The residue samples for SEM were collected after combustion in the vertical burning tests and sputter-coated with a thin layer of gold on the surfaces before SEM tested.

Mechanical Properties Measurements. For the measurements of tensile properties, dumbbell-shape specimens were prepared and tested on a universal testing machine (Instron 4465, Instron) according to ASTM D412. All tests were performed at room temperature and the average value was calculated for at least five test specimens.

RESULTS AND DISCUSSION

FTIR Analysis of MP

MP was synthesized by reacting melamine with phosphoric acid (shown in Scheme 1).[13] Figure 1 shows the FTIR spectrum of home-made MP. According to the reference,[14] the typical peak of MP (listed in Table I) can be found, including 3398 cm^{-1} and 3154 cm^{-1} (asymmetric and symmetric NH stretch), 2682 cm^{-1}, 1245 cm^{-1}, and 959 cm^{-1} (O═P—O—H), 1670 cm^{-1} (C═N and NH_2), and so on, which confirms the successful synthesis of MP.

Flammability Properties

The LOI values and vertical burning ratings (UL-94) of various samples with different compounding ratios are given in Table II. For OBC/MPPER system (Sample MPPER-1–9), all samples were easily flammable materials with low LOI values (less than 25) and no rating in UL-94 test, except the sample MPPER-5 with a 50 wt % loading of MPPER (MP : PER = 1 : 1 wt : wt), which reached UL-94 V-0 rating with a LOI value of 30.5. It was also found that, at the same IFR loading (i.e., 40 wt %), the materials had the highest LOI value when the weight ratio of MP to PER was 3 : 2 (Sample MPPER-7), indicating that the

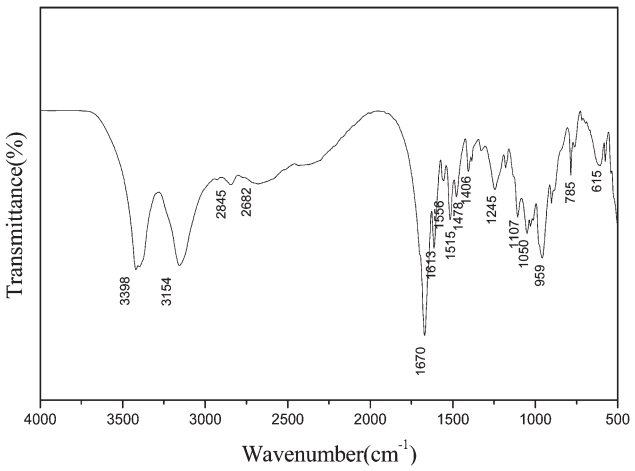

Figure 1. The FTIR spectrum of home-made MP.

MPPER IFR system in OBC exhibited the highest efficiency at this weight ratio.

Although polyamide 6 (PA6) can act as a carbon source in IFR and enhance the flame retardancy of materials by compounding with other carbon sources,[15,16] its melt temperature is 235°C, which is not compatible with the processing temperature of OBC (less than 200°C). PA12 has the similar molecular components with PA6 and a much lower melt temperature (178°C). So PA12 was introduced into the OBC/MPPER systems (Sample MPPER-PA-1–7). The weight ratio of MP to carbon source (PER+PA12) was kept in 1 : 1. It was found that the addition of PA12 enhanced the flame retardancy obviously. Especially, Sample MPPER-PA-4 passed the UL-94 V-0 test with a LOI value of 29.3 as shown in Table II.

$NiCO_3{\cdot}2Ni(OH)_2{\cdot}4H_2O$ and La_2O_3 were added as synergistic agents in IFR (Sample MPPER-Ni-1–7 and Sample MPPER-La-1–7). The weight ratio of MP to PER was kept in 3 : 2. It was found that all the MPPER-Ni and MPPER-La samples reached UL-94 V-0 rating and the LOI values were 28.5, even if the addition of $NiCO_3{\cdot}2Ni(OH)_2{\cdot}4H_2O$ and La_2O_3 was as low as 0.5 phr in 100 phr OBC/MPPER, which indicates a good synergistic effect of $NiCO_3{\cdot}2Ni(OH)_2{\cdot}4H_2O$ or La_2O_3 with MPPER in IFR.

Although EG is known to be a very efficient IFR additive that performs both as a carbon source and as a gas source[10]; however, a large loading of EG (40 wt % for sample EG-4) was required at a UL-94 V-0 lever. EG system was reported to have a better flame-retardant efficiency when combined with other IFR,[17] which was proved in our OBC-IFR system (Sample MPPER-EG-0–7). For OBC/MPPER systems at MP : PER = 3 : 2 wt : wt, and the total loading of MPPER/EG of 30 wt %, the samples can reach UL-94 V-0 rating when the loading of EG was 15–18 wt % (Sample MPPER-EG-5 and 6). The compounding of EG and MPPER improved the flame-retardant efficiency and lowered the loading of flame retardants in OBC.

Thermal Stability

Figure 2 shows the TGA and derivate thermogravimetric (DTG) curves of the samples. Correspondingly, the temperatures, at which the relative mass loss is 10% ($T_{10\%}$) and 50% ($T_{50\%}$), respectively, were obtained from TGA curves and listed in Table III. The decomposition peak temperatures of T_{250}, T_{30}, and T_{480}, shown at about 250°C, 430°C, and 480°C, respectively, on the DTG curves in Figure 2, alone with the values of char residue were also given in Table III.

It can be found that the thermal degradation of pure OBC occurred at 425°C and that almost no char residue was left [Figure 2(a), Table III]. The introduction of MPPER improved the char residue remarkably and had an obvious effect on the thermal degradation behavior of OBC-IFR composites which degraded in two steps. The first step initiated at around 225°C and the second step began at about 425°C. In the first step, MP reacted with PER to form esters and water (225–300°C). With temperature increasing, the esters decomposed to release ammonia and then crosslinked with OBC to form char layers (300–425°C). Because of the released gas, such as ammonia and water vapor, the char layers had swollen multicellular structures, which can protect the materials from flame and increase the char residue. The second step at 425°C corresponds to the degradation of OBC.

According to the TGA and DTG curves in Figure 2(b), it can be found that the addition of PA12 in OBC/MPPER composites improved the thermal stabilities of materials obviously. The initial decomposition temperature increased with the content of PA12. The small peaks between 375 and 450°C in DTG curves indicated that, as a carbon source, PA12 reacted and decomposed at a higher temperature than PER did. However, the char residue slightly decreased with the increase of PA12 content as shown in Table III, indicating that the flame-retardant effect became poor when the addition of PA12 was more than 6.4 wt %. This can be attributed to that the reactivity of PA12 was lower than the small molecules of PER and less cross-linked char layers formed in the presence of PA12. The charring mechanism of MP/PA12 is shown in Scheme 2. In a word, PA12 improved the thermal stabilities, but lowered the charring abilities of IFR. With the effect of the two opposite aspects, MPPER-PA-7 had a higher LOI value than MPPER-4.

As shown in Figure 2(c,d), with the addition of $NiCO_3{\cdot}2Ni(OH)_2{\cdot}4H_2O$ and La_2O_3, the curves of TGA move to a lower temperature. The shift of the curves suggested that

Table I. Assignment of FTIR Absorption Bands of MP

Band position (cm^{-1})	Assignment
3398, 3154	Asymmetric and symmetric NH stretch
2682, 1245, 959	typical of O=P–O–H
1670	C=N stretch + NH_2 deformation
1613, 1556, 1515, 1478, 1406	ring stretch
1107, 1050	PO_2^- stretch
785	Ring deformation
615	NH_2 deformation

Table II. Formulations and Characterizations of OBC-IFR Various Systems

	Compositions(g)								Characterizations			
Sample	OBC 9817	OBC 9000	MP	PER	PA12	$NiCO_3 \cdot 2Ni(OH)_2 \cdot 4H_2O$	La_2O_3	EG	UL-94	LOI	Tensile strength (MPa)	Elongation at break (%)
MPPER-0	100								NR	19.2	3.6	1540
MPPER-1	90		5	5					NR	19.7	3.5	1370
MPPER-2	80		10	10					NR	21.3	3.3	1230
MPPER-3	70		15	15					NR	23.8	3.0	1160
MPPER-4	60		20	20					NR	24.5	2.4	1080
MPPER-5	50		25	25					V-0	30.5	1.7	740
MPPER-6	60		30	10					NR	24.5		
MPPER-7	60		24	16					NR	25.0	2.6	1170
MPPER-8	60		16	24					NR	23.8		
MPPER-9	60		10	30					NR	22.3		
MPPER-PA-1	60		20	18.4	1.6				V-1	26.5	2.5	1140
MPPER-PA-2	60		20	16.8	3.2				V-1	27.2	2.6	1160
MPPER-PA-3	60		20	15.2	4.8				V-1	28.0	2.8	1170
MPPER-PA-4	60		20	13.6	6.4				V-0	29.3	2.9	1090
MPPER-PA-5	60		20	12	8				V-1	27.5	3.0	970
MPPER-PA-6	60		20	10.4	9.6				V-1	26.8	3.2	930
MPPER-PA-7	60		20	8.8	11.2				V-2	26.0	3.4	790
MPPER-Ni-1	60		24	16		0.5			V-0	28.5	2.1	1100
MPPER-Ni-2	60		24	16		1			V-0	28.8	2.1	1050
MPPER-Ni-3	60		24	16		1.5			V-0	29.0	2.1	1030
MPPER-Ni-4	60		24	16		2			V-0	29.0	2.1	1010
MPPER-Ni-5	60		24	16		2.5			V-0	28.5	2.1	980
MPPER-Ni-6	60		24	16		3			V-0	28.5	2.1	950
MPPER-Ni-7	60		24	16		3.5			V-0	28.5	2.1	870
MPPER-La-1	60		24	16			0.5		V-0	28.5	2.0	1050
MPPER-La-2	60		24	16			1		V-0	29.7	2.0	1030
MPPER-La-3	60		24	16			1.5		V-0	30.0	2.0	1000
MPPER-La-4	60		24	16			2		V-0	29.3	2.0	980
MPPER-La-5	60		24	16			2.5		V-0	28.5	2.0	940
MPPER-La-6	60		24	16			3		V-0	28.0	2.0	900
MPPER-La-7	60		24	16			3.5		V-0	27.8	2.0	810
EG-0		100							NR	19.7	6.3	1310
EG-1		90						10	NR	21.5	6.0	1180
EG-2		80						20	NR	22.7	6.0	1110
EG-3		70						30	V-2	29.3	6.0	1050
EG-4		60						40	V-0	33.0	5.8	910
MPPER-EG-0		70	18	12					NR	23.3	5.0	1210
MPPER-EG-1		70	16.2	10.8				3	NR	22.5	5.0	1190
MPPER-EG-2		70	14.4	9.6				6	NR	23.0	5.0	1250
MPPER-EG-3		70	12.6	8.4				9	NR	24.5	5.0	1200
MPPER-EG-4		70	10.8	7.2				12	V-2	26.8	5.2	1180
MPPER-EG-5		70	9	6				15	V-0	28.5	5.3	1140
MPPER-EG-6		70	7.2	4.8				18	V-0	30.0	5.5	1170
MPPER-EG-7		70	5.4	3.6				21	V-2	27.8	5.8	1150

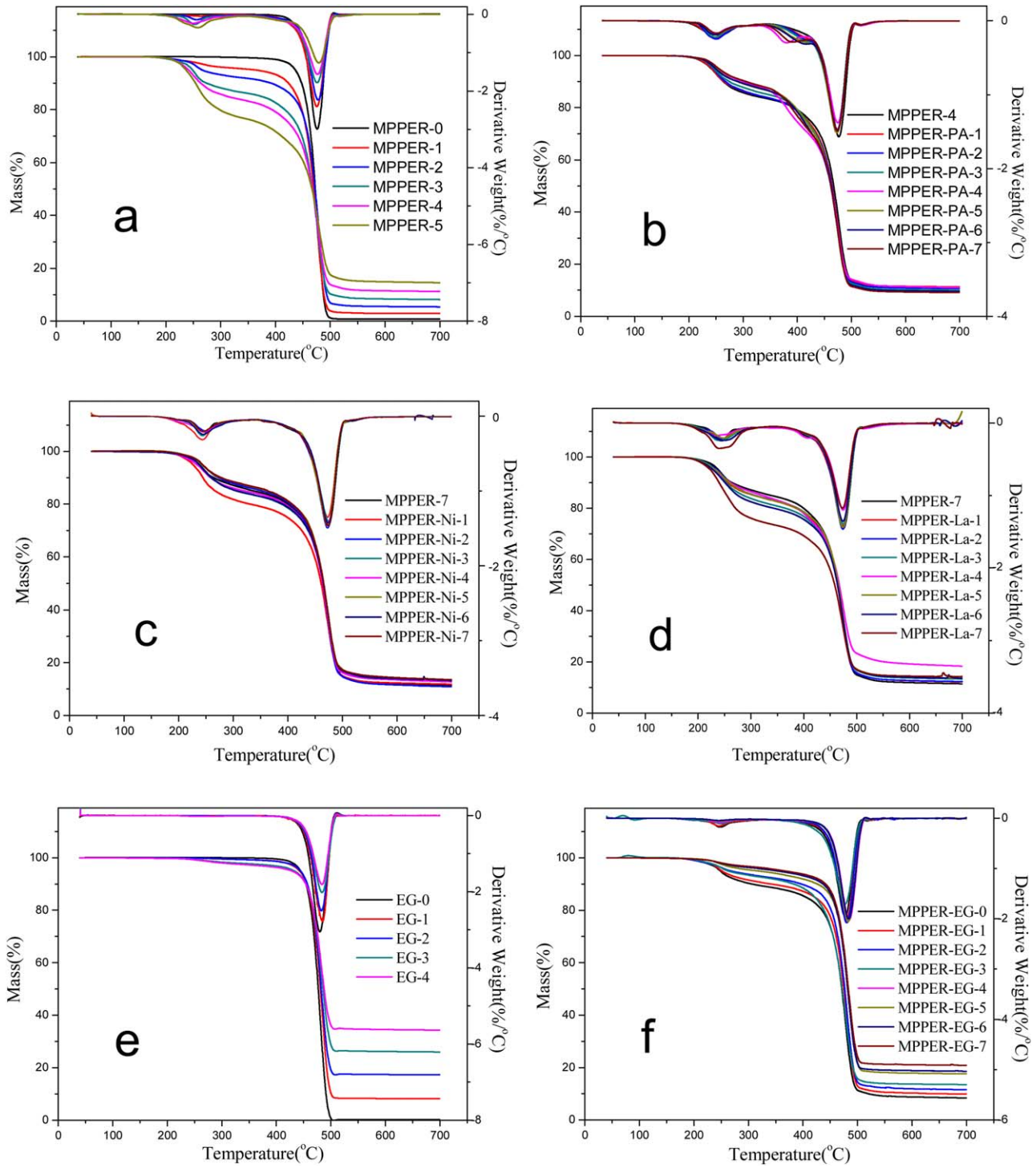

Figure 2. TGA and DTG curves of (a) MPPER, (b) MPPER-PA, (c) MPPER-Ni, (d) MPPER-La, (e) EG, and (f) MPPER-EG samples. [Color figure can be viewed in the online issue, which is available at wileyonlinelibrary.com.]

$NiCO_3 \cdot 2Ni(OH)_2 \cdot 4H_2O$ and La_2O_3 promoted the catalytic esterification of IFR and accelerated the reaction speed of esterification. Besides this, the char residue increased in the presence of $NiCO_3 \cdot 2Ni(OH)_2 \cdot 4H_2O$ and La_2O_3, indicating that the carbonaceous formation was also improved. Compared with $NiCO_3 \cdot 2Ni(OH)_2 \cdot 4H_2O$, the effect of La_2O_3 on catalytic action of IFR is strong.

As shown in Figure 2(e,f), and in Table III, the addition of EG can improve the char residue a lot. Slight mass loss can be observed between 250 and 425°C corresponding to the releasing of non-flaming gas in EG. For MPPER-EG samples, the addition of EG also improved the thermal stabilities of materials.

Table III. The Values of $T_{\%}$, the Decomposition Peak Temperatures on DTG Curves, and Char Residue

Samples	$T_{10\%}$ (°C)	$T_{50\%}$ (°C)	T_{250} (°C)	T_{430} (°C)	T_{480} (°C)	Char residue (wt %)
MPPER-0	448	473	-	-	477	0.9
MPPER-1	424	470	263	-	476	2.9
MPPER-2	393	472	256	-	478	5.4
MPPER-3	274	468	253	-	477	8.2
MPPER-4	264	467	250	-	477	11.2
MPPER-5	254	467	258	-	480	14.5
MPPER-PA-1	264	467	250	-	477	11.3
MPPER-PA-2	265	464	249	426	475	10.7
MPPER-PA-3	268	464	251	428	475	10.1
MPPER-PA-4	274	462	248	429	473	11.0
MPPER-PA-5	299	462	249	430	475	9.5
MPPER-PA-6	290	462	248	431	474	9.6
MPPER-PA-7	290	462	248	431	475	9.1
MPPER-Ni-1	245	461	245	-	475	11.8
MPPER-Ni-2	249	464	244	-	474	11.9
MPPER-Ni-3	260	465	245	-	473	13.1
MPPER-Ni-4	258	464	244	-	475	12.8
MPPER-Ni-5	259	464	245	-	475	13.5
MPPER-Ni-6	259	465	243	-	473	13.3
MPPER-Ni-7	258	465	246	-	475	13.5
MPPER-La-1	256	464	245	-	475	12.2
MPPER-La-2	260	465	240	-	474	12.3
MPPER-La-3	252	465	244	-	475	13.3
MPPER-La-4	260	467	239	-	476	18.4
MPPER-La-5	259	466	230	-	475	14.4
MPPER-La-6	251	464	245	-	475	13.6
MPPER-La-7	240	458	242	-	475	13.2
EG-0	454	477	-	-	481	0.9
EG-1	455	481	-	-	484	8.2
EG-2	456	482	-	-	483	17.3
EG-3	456	485	-	-	484	26.0
EG-4	456	488	-	-	484	34.3
MPPER-EG-0	305	471	248	-	478	8.4
MPPER-EG-1	338	475	245	-	481	9.9
MPPER-EG-2	398	477	248	-	481	11.5
MPPER-EG-3	382	472	249	-	478	13.4
MPPER-EG-4	427	483	247	-	485	17.6
MPPER-EG-5	437	482	246	-	483	17.6
MPPER-EG-6	441	483	245	-	484	18.6
MPPER-EG-7	305	471	248	-	478	20.8

Morphologies

Figures 3–6 show the SEM micrographs of the char residue of various samples. For OBC/MPPER system (Figure 3), when the loading of MPPER (MP : PER = 1 : 1 wt : wt) was less than 50 wt % (Sample MPPER-4 and MPPER-7), the samples were easily flammable and no rating in UL-94 test. The char residue structures of Sample MPPER-4 [Figure 3(a)] and MPPER-7 [Figure 3(c)] looked very loose with lots of holes, which is conducive to the oxygen and heat transfer, and makes the materials burn easily. When the loading of MPPER reached 50 wt % (Sample MPPER-5), the sample [Figure 3(b)] displayed more condensed structure than Sample MPPER-4 and MPPER-7, which results in a higher LOI and passing UL-94 V-0 test.

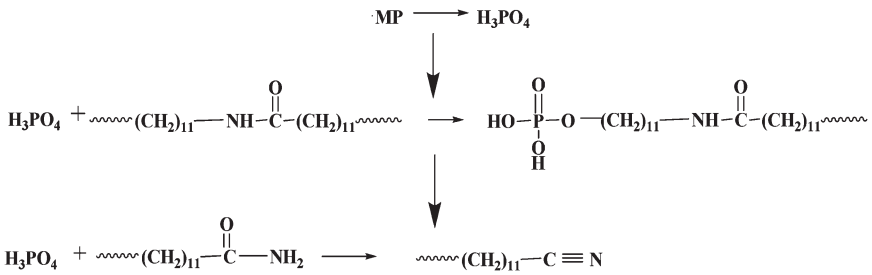

Scheme 2. The charring mechanism of MP/PA12.

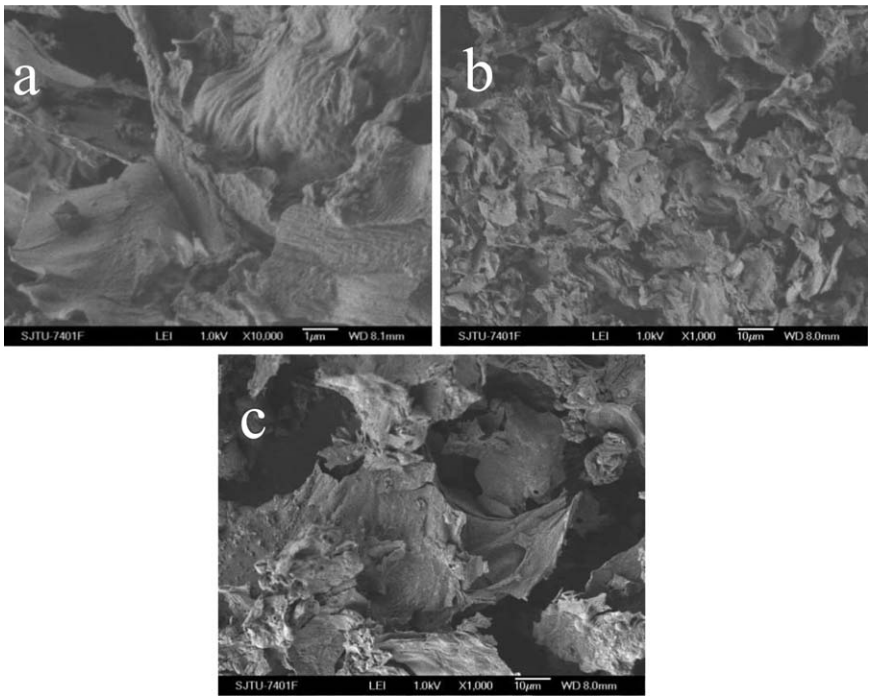

Figure 3. SEM micrographs of the char residue of (a) MPPER-4, (b) MPPER-5, and (c) MPPER-7 after burning.

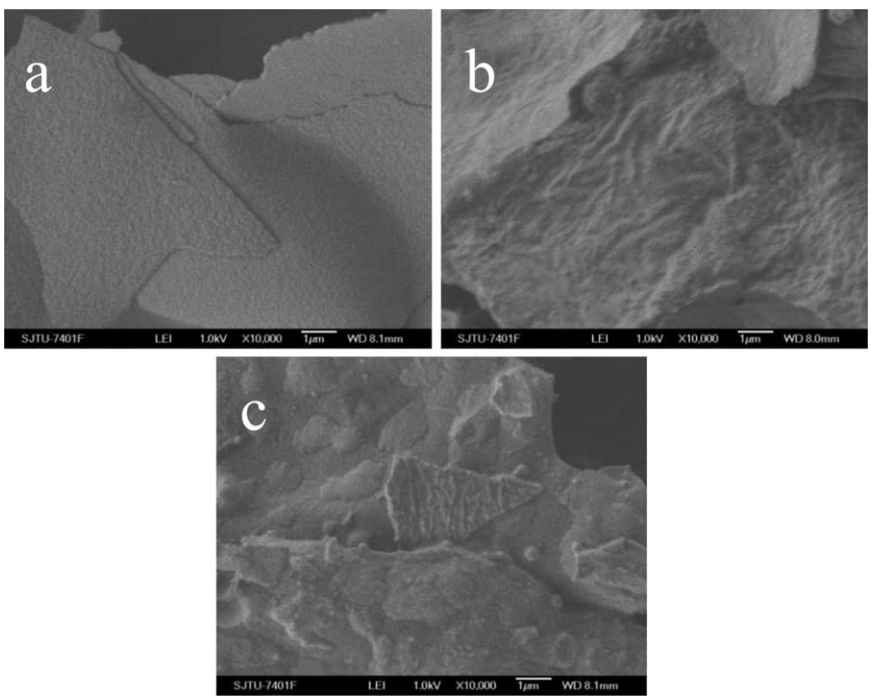

Figure 4. SEM micrographs of the char residue of (a) MPPER-PA-2, (b) MPPER-PA-4, and (c) MPPER-PA-7 after burning.

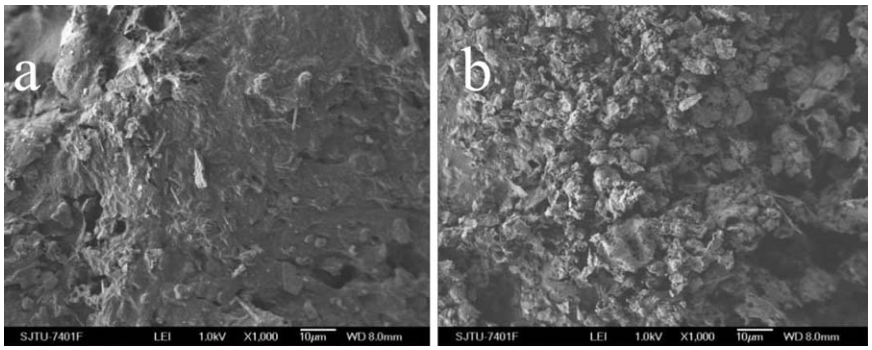

Figure 5. SEM micrographs of the char residue of (a) MPPER-Ni-5 and (b) MPPER-La-5 after burning.

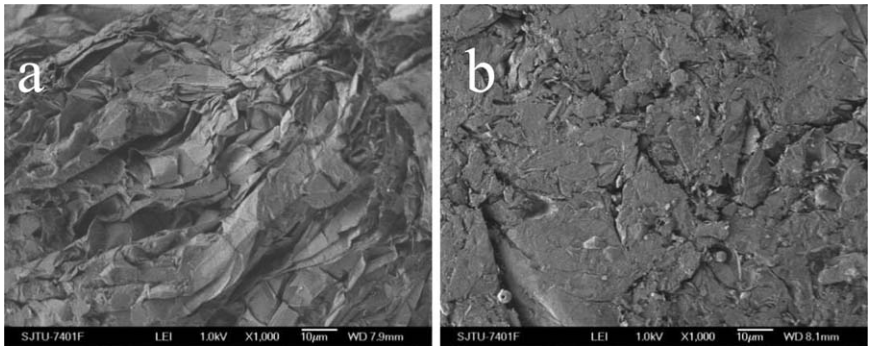

Figure 6. SEM micrographs of the char residue of (a) EG-4 and (b) MPPER-EG-6 after burning.

For OBC/MPPER/PA12 system (Figure 4), PA12 can act as a carbon source and compound with MP when the weight ratio of MP to carbon source (PER + PA12) was kept in 1 : 1. The presence of PA12 helped Sample MPPER-PA-4 form smooth and compact char layers [Figure 4(b)], which can isolate oxygen well and thereby improve the flame retardant performance. When the PA12 content was as low as 3.2 wt % (Sample MPPER-PA-2), the char layers looked too thin to insulate heat flow [Figure 4(a)], leading to a failure in passing UL-94 V-0 tests. When the PA12 content was as high as 11.2 wt % (Sample MPPER-PA-7), the low reactivity of PA12 leaded less cross-linked char layers formed [Figure 4(c)] resulting in a setback in flame retardancy.

Figures 5 and 6 show the SEM micrographs of the char residue of the Sample MPPER-Ni-5, MPPER-La-5, EG-4, and MPPER-EG-6. All of them have thick and compact char residue structures, indicating a good synergistic effect between the additives and MPPER, which is in a good agreement with the results of flammability tests.

Tensile Properties

Tensile strength and elongation at break of the OBC-IFR composite samples as a function of the content of MPPER in OBC9817 and EG in OBC9000 are shown in Figure 7. It is obvious that the addition of MPPER and EG in OBC decreased

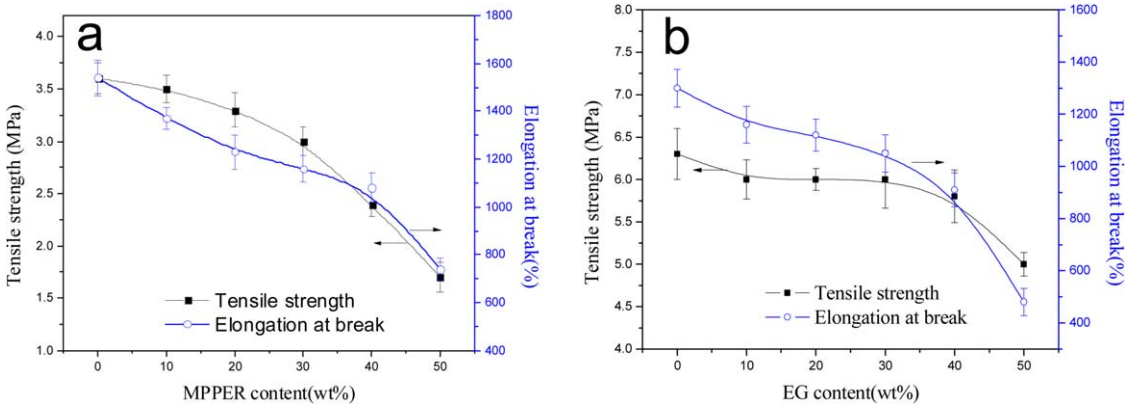

Figure 7. Tensile strength and elongation at break of the composite samples as a function of the content of (a) MPPER in OBC 9817 and (b) EG in OBC 9000. [Color figure can be viewed in the online issue, which is available at wileyonlinelibrary.com.]

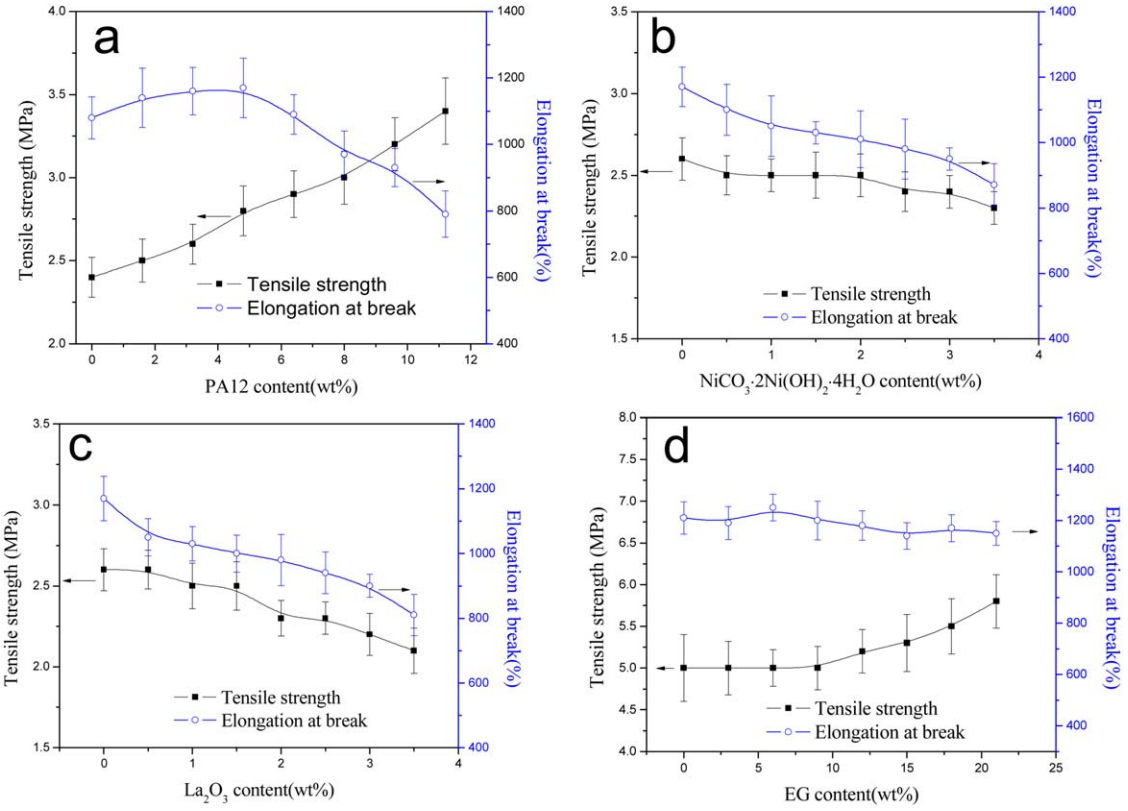

Figure 8. Tensile strength and elongation at break of the composite samples shown in Table II as a function of the content of (a) PA12 in Samples MPPER-PA, (b) NiCO3·2Ni(OH)2·4H2O in Samples MPPER-Ni, (c) La2O3 in Samples MPPER-La, and (d) EG in Samples MPPER-EG. [Color figure can be viewed in the online issue, which is available at wileyonlinelibrary.com.]

the tensile strength and elongation at break of materials simultaneously, which is attributed to the poor compatibility and dispersion of these inorganic additives in OBC matrix. For MPPER, there was a 52% decrease in tensile strength and 51.9% decrease in elongation at break when the loading of MPPER was 50 wt %. For EG, there was a 7.9% decrease in tensile strength and 30.5% decrease in elongation at break when the loading of MPPER was 40 wt %, which indicates that EG has less setback in mechanical properties of materials than MPPER, especially in tensile strength.

Figure 8 shows the tensile strength and elongation at break of the composite samples shown in Table II as a function of the content of additives in each corresponding samples. PA12 has a better compatibility with OBC than the inorganic additives and a worse elasticity than OBC. So the addition of PA12 increased the tensile strength but decreased the elongation at break of materials [Figure 8(a)]. In comparison with pure OBC9817, there was a 19.4% decrease in tensile strength and 29.2% decrease in elongation at break for Sample MPPER-PA-4, which can pass the UL-94 V-0 test. Because of the poor compatibility and dispersion of $NiCO_3{\cdot}2Ni(OH)_2{\cdot}4H_2O$ and La_2O_3, the addition of metallic compounds decreased both tensile strength and elasticity [Figure 8(b,c)]. There was a 41.6% and 44.44% decrease in tensile strength and 28.6% and 31.8% decrease in elongation at break for Sample MPPER-Ni-1 and MPPER-La-1, respectively. For Samples MPPER-EG, the increase of EG content improved the tensile strength and almost had no influence on elongation at break of materials, which indicates that EG had a better dispersion than MPPER in OBC and has a good agreement with Figure 7, although both of them weaken the mechanical properties of materials. In comparison with pure OBC9000, there was a 12.7% decrease in tensile strength and 10.7% decrease in elongation at break for Sample MPPER-EG-6, which can pass the UL-94 V-0 test. Mechanical performance of the samples shown in Figures 7 and 8 suggested that the loading of IFR additives used in this work can improve effectively the flame retardancy of the OBC at the cost of the mechanical properties of TPEs. For some OBC-IFR systems (i.e., MPPER-EG system), when using suitable loading of IFR, the TPEs with a tolerable decrease in mechanical properties can be maintained.

CONCLUSION

OBC without addition of flame retardants are readily flammable materials. The addition of MPPER made OBC pass the UL-94 V-0 test only if the content of MPPER was more than 50 wt %, nevertheless giving rise to a serious decrease in the mechanical properties of the materials.

The loading of suitable amount of IFR used in this work can improve effectively the flame retardancy of the OBC. PA12 in OBC/MPPER system can enhance the flame retardancy and

tensile strength of the materials concurrently. The materials could pass the UL-94 V-0 test when the loading of PA12 was 6.4 wt % and MPPER was 33.6 wt %. Both $NiCO_3{\cdot}2Ni(OH)_2{\cdot}4H_2O$ and La_2O_3 had a strong catalytic action in improving the carbonaceous formation of MPPER system and enhanced the flame retardancy of OBC/MPPER composites significantly even if the loading of them was as low as 0.5 phr, which only caused a less decrease in the mechanical property. While the OBC/EG system could pass the UL-94 V-0 test when the loading of EG was 40 wt %, the addition of EG at the amount of 15–18 wt % to MPPER system lowered the total loading of flame retardants in OBC to 30 wt % at the same flame-retardant level.

ACKNOWLEDGMENTS

The authors are thankful for the financial support for this work from the National Basic Research Program of China (2011CB606005 and 2012CB025901), National Natural Science Foundation of China (51103084), and the Shanghai Leading Academic Discipline Project (No. B202).

REFERENCES

1. Xiao, W. D.; Kibble, K. A. *Polym. Polym. Compos.* **2008**, *16*, 415.
2. Lu, H. D.; Si, J. Y.; Zhao, D. F.; Wu, H. T.; Ma, Y. Q.; He, H. *Asian J. Chem.* **2012**, *24*, 4056.
3. Lai, X. J.; Zeng, X. R.; Li, H. Q.; Liao, F.; Zhang, H. L.; Yin, C. Y. *J. Macromol. Sci. B* **2012**, *51*, 35.
4. Qiao, Z. H.; Tai, Q. L.; Song, L.; Hu, Y.; Lv, P.; Jie, G. X.; Huang, W.; Fu, Y.; Zhang, D. Q. *Polym. Adv. Technol.* **2011**, *22*, 2602.
5. Ma, H. Y.; Tong, L. F.; Xu, Z. B.; Fang, Z. P. *Appl. Clay Sci.* **2008**, *42*, 238.
6. Wang, X.; Feng, N.; Chang, S. Q.; Zhang, G. X.; Li, H.; Lv, H. *J. Appl. Polym. Sci.* **2012**, *124*, 2071.
7. Yin, H. Q.; Yuan, D. D.; Cai, X. F. *J. Therm. Anal. Calorim.* **2013**, *111*, 499.
8. Demir, H.; Arkis, E.; Balkose, D.; Ulku, S. *Polym. Degrad. Stabil.* **2005**, *89*, 478.
9. Lin, M.; Li, B.; Li, Q. F.; Li, S.; Zhang, S. Q. *J. Appl. Polym. Sci.* **2011**, *121*, 1951.
10. Han, J. P.; Liang, G. Z.; Gu, A. J.; Ye, J. H.; Zhang, Z. Y.; Yuan, L. *J. Mater. Chem. A* **2013**, *1*, 2169.
11. Arriola, D. J.; Carnahan, E. M.; Hustad, P. D.; Kuhlman, R. L.; Wenzel, T. T. *Science* **2006**, *312*, 714.
12. Jin, J.; Du, J. A.; Xia, Q. H.; Liang, Y. R.; Han, C. C. *Macromolecules* **2010**, *43*, 10554.
13. Liu, M. F.; Liu, Y.; Wang, Q. *Macromol. Mater. Eng.* **2007**, *292*, 206.
14. Balabanovich, A. I. *Thermochim. Acta* **2005**, *435*, 188.
15. Almeras, X.; Dabrowski, F.; Le Bras, M.; Delobel, R.; Bourbigot, S.; Marosi, G.; Anna, P. *Polym. Degrad. Stabil.* **2002**, *77*, 315.
16. Almeras, X.; Dabrowski, F.; Le Bras, M.; Poutch, F.; Bourbigot, S.; Marosi, G.; Anna, P. *Polym. Degrad. Stabil.* **2002**, *77*, 305.
17. Xie, R. C.; Qu, B. J. *J. Appl. Polym. Sci.* **2001**, *80*, 1190.